



## A QUALITY BY DESIGN CONCEPT ON POLYMER BASED NANOPARTICLES CONTAINING ANTI-ALZHEIMER'S DRUG

G. Ravi, N. Vishal Gupta<sup>1</sup>, Valluru Ravi\*, P. Subhash Chandra Bose, Damineni Sarita<sup>2</sup>

Department of Pharmaceutics, MNR College of Pharmacy, MNR Educational Trust, MNR Nagar, Sangareddy-502294, Telangana State, India.

<sup>1</sup>Department of Pharmaceutics, JSS College of Pharmacy, Sri Shivarathreeshwara Nagar, Mysuru, Jagadguru Sri Shivarathreeshwara University, Sri Shivarathreeshwara Nagar, Mysuru-570015, Karnataka, India.

<sup>2</sup>Department of Pharmaceutics, Sultan-ul-Uloom College of Pharmacy, Hyderabad, Telangana State, India.

\*Corresponding author E-mail: [vallururavi26@gmail.com](mailto:vallururavi26@gmail.com)

### ARTICLE INFO

### ABSTRACT

**Key Words:**  
Alzheimer's disease;  
Rivastigmine Tartrate;  
Polymeric nanoparticles;  
Glycol Chitosan



The objective of this investigation was to prepare polymeric nanoparticles (PNPs) of Rivastigmine Tartrate and to characterize the physicochemical properties of PNPs. A series of PNPs were prepared by modified solvent emulsification diffusion technique using polymer, surfactant and solvents. Zeta potential of optimized formulation was found to be +35.81 mV indicating stable formulation. The particle size of nanoparticles was found in the range of 247±15 to 459±11 nm. The PDI of all formulations was found to be in the range of 0.374-0.719, which concluded that prepared nanoparticle was mono dispersed in nature. Entrapment efficiency of nanoparticles was found in the range of 41.62 ± 1.5 to 51.47 ± 1.8%. The drug release at 24<sup>th</sup> hour was found in the range of 86.72±0.97 to 97.81±0.26% for various formulations. We concluded that Glycol Chitosan nanoparticles have the potential to be used as smart carriers to deliver Rivastigmine Tartrate to brain cells.

### INTRODUCTION:

The neurodegenerative disorders (NDs) consist of various conditions that steadily reduce patient memory and cognition in the elderly population. Alzheimer's disease (AD) is considered as one of the major progressive socio-economical and medical burden around the world [1]. The etiology of AD is not clear and the factors that are considered to play a vital role in its pathogenesis include reduced acetylcholine levels, abnormal proteins,

excessive accumulation and oxidative stress [2]. The major factor that hold back for the discovery of the drugs and in effective development of delivery system for the cure and prevention of AD is due to existence of blood brain barrier (BBB) which obstruct anti Alzheimer's drug to brain [3]. The drug diffusion across BBB from blood, build upon the physicochemical properties such as positive charge, low molecular weight and

lipid solubility. In overcoming the difficulty different strategies are developed to improve the drug availability to the brain.

In recent years, drug delivery systems targeting brain has developed interest in researchers has lead to the fabrication of several colloidal carriers such as liposomes [4], polymeric nanoparticles (PNPs) [5], solid lipid nanoparticles (SLNs) [6], and dendrimers [7]. In Nano carriers PNPs are found to be talented carrier with the ability to open up BBB tight junctions (Tj). They can in fact cover the membrane barrier and prevent the drug molecule characterization to prolong drug release and protects from enzymatic degradation. Nanoparticles prepared out of hydrophilic polymers like chitosan shows superiority in prolonging circulation and nanoparticles with in the particle size range of less than 200 nm avoids opsonisation [8-10].

Glycol chitosan, a water soluble derivative [11] feel bound to its water soluble capacity and helps in absorption of the hydrophilic glycol group. Importantly, the free amine groups on the backbone would be helpful for further alteration or interface with the host cells. Even though a very little characterization has been conducted to explain glycol chitosan's real structure, it is proposed for being a suitable material in several pharmaceutical and biomedical applications. Rivastigmine Tartrate is used is chemically (2R,3R)-2, 3-dihydroxybutanedioic acid; 3-[(1S)-1-(dimethylamino)ethyl]phenyl N-ethyl-N-methylcarbamate, the precise mechanism of Rivastigmine has not been fully determined, but it is suggested that rivastigmine binds reversibly and inactivates cholinesterase (eg. acetylcholinesterase, butyrylcholinesterase), preventing the hydrolysis of acetylcholine, and thus leading to an increased concentration of acetylcholine at cholinergic synapses. The anti cholinesterase activity of Rivastigmine is relatively specific for brain acetyl cholinesterase and butyryl cholinesterase

compared with those in peripheral tissues. It has very short half life (1.5 h), low bioavailability (36%) [12].

Quality by Design (QbD) is defined in ICH guidelines Q8(R2) as “A systematic approach to development that begins with predefined objectives and emphasizes product and process understanding and process control, based on sound science and quality risk management” [13].

## 2. MATERIALS & METHODS:

### 2.1 MATERIALS:

Rivastigmine Tartrate was obtained as a gift sample from Jubilant life sciences Ltd, India. Glycol chitosan was purchased from Sigma-Aldrich, USA. Poloxamer 188 was purchased from BASF, Germany. Propylene glycol was procured from Loba chemie, Mumbai, India. All other solvents, reagents and chemicals used were of analytical grade.

### 2.2. QUALITY BY DESIGN

The development strategy follows Quality by Design (QbD) principles and can be divided into the five steps

#### 2.2.1. QTPP (Quality Target Product Profile)

Quality characteristics of a drug product that ideally will be achieved to ensure the desired quality, taking into account safety & efficacy of the drug product [14].

#### 2.2.2. CQA (Critical Quality Attributes)

The most critical Quality Attributes [15] that affect the nanoparticles identified factors are listed in Table 1.

##### 2.2.2.1. Risk Assessment

Risk assessment consists of the identification of hazards, analysis and evaluation of risks associated with exposure to those hazards. Quality risk assessments begin with a well-defined problem description or risk question. When the risk in question is well defined, an appropriate risk management tool and the types of information needed to address the risk question will be more readily identifiable. In an early risk assessment the critical parameters should be identified

that could be method factors which may affect sample separation as well as settings in the instrumental analysis. In the present investigation with target as faster and clear separation of 1 drug the risk assessment through the cause and effect model was used to identify the potential risk. The process parameters and material attributes that exhibits risks and can affect the particle size, entrapment efficiency and drug release. Further the risks were ranked according to its potential to affect the desired targets [16].

### 2.2.2.2 Design of Experiments

The formulations designed by Design-Experiment Software 10 version

## 2.3. PREFORMULATION STUDY FOR DRUG AND PHYSICAL MIXTURE

### 2.3.1 Fourier Transform Infrared Spectroscopy (FT-IR) Analysis

Drug and excipients interactions can be detected by FTIR spectroscopy by following the shift in vibrational and stretching bands of key functional groups. The spectra were acquired by diffuse reflectance on a FTIR spectrophotometer (Shimadzu FTIR-8400 spectrophotometer). The samples were prepared by KBR pellet method, where the test samples were dispersed in potassium bromide (KBR) powder, pelletized and analyzed. Scanning of spectra was done over a number range of 4000-400  $\text{cm}^{-1}$  [17].

**Table 1. Critical Quality Attributes for PNP**

Critical Quality Attributes for PNP			
Quality Attribute	Target	CQAs	Justification
Particle Size (nm)	200-400	Yes	For better absorption and enhancing the bioavailability
Entrapment Efficiency (%)	40-70	Yes	To determine the amount of drug present in the dosage form in the soluble state
Drug Release (%)	85-100	Yes	To determine the percentage of drug released from the dosage form into external buffer medium

### 2.3.2. DIFFERENTIAL SCANNING CALORIMETRY (DSC)

A commonly used thermo-analytical method to generate data on glass transitions and melting endotherms is DSC. All dynamic DSC studies were carried out on DuPont thermal analyzer with 2010 DSC module. 3-4 mg of test samples were captured and sealed hermetically in flat-bottomed aluminum pan with lid crimped, followed by positioning these pans on a sample pan holder. Samples were equilibrated for a minute and later heated in a nitrogen atmosphere over 0-240 °C temperature

range with 10 °C/min heating rate. Empty aluminum pan served as reference. At the flow rate of 20 ml/min, nitrogen was used as purge gas for all studies [18].

### 2.4. PREPARATION OF PNP

PNPs of Rivastigmine Tartrate were prepared by modified solvent emulsification diffusion method. The drug was dissolved in distilled water (internal phase). Small quantity of surfactant (poloxamar 188) and required quantity of polymer (Glycol chitosan) were dissolved in 10 ml of distilled water and heated for 10 minutes and propylene glycol was

added to stearic acid solution (external phase). External phase was added to internal phase solution and 10 ml of 70 % aqueous ethanol (co-solvent) and tween 80 (stabilizer) was added to above solution and the mixture was homogenized (PolytronPT 1600E, Switzerland) for 15 min at 2000 g, and sonicated (Vibra Cell, Model VCX 750, Connecticut, USA) for 10 min. The organic solvents were removed by evaporation at 40 °C under normal pressure, and the nanoparticles were separated by using cooling centrifuge (REIL, C-24 BL) for 15 min at 10000 rpm. Supernatant liquid was removed and nanoparticles were washed with distilled water and freeze dried (REMI Ultra low freezer, UDFV-90) using mannitol as cryoprotectant [19].

#### 2.4.1. Experimental Design

A randomized, 3<sup>2</sup> full factorial designs with 2 factors at 3 levels was used to study the formulation of PNPs. Nine experimental trials were conducted at all possible combinations. The amount of glycol chitosan and poloxamer 188 (surfactant) were chosen as independent variables. The particle size, entrapment efficiency and % cumulative drug release at 24<sup>th</sup> h were used as dependent variables (responses). Design-Expert 10.0 software (Stat-Ease Inc., USA) was used for generation and evaluation of the statistical experimental design [20-22]. The matrix of 3<sup>2</sup> factorial design obtained from the study is represented in Table 2.

**Table 2.** Matrix of 3<sup>2</sup> factorial designs for Rivastigmine Tartrate PNPs

Run	Factors	
	Polymer (%)	Surfactant (%)
RP1	0.2	0.04
RP2	0.4	0.04
RP3	0.4	0.03
RP4	0.2	0.02
RP5	0.3	0.04
RP6	0.2	0.03
RP7	0.4	0.02
RP8	0.3	0.02
RP9	0.3	0.03

## 2.5. Characterization of PNPs

### 2.5.1. Size measurement and polydispersity index

The size of drug particles and PDI were determined by using Zetasizer Nano ZS (Malvern Instruments, Malvern, UK). A pre weighed amount of sample was dispersed in demineralized water was placed directly into the module and the data was collected. The studies were performed at room temperature. All the samples were analyzed in triplicate [23].

### 2.5.2. Scanning Electronic Microscopy (SEM)

The morphology of the formulations was determined using a scanning electron microscope (Hitachi S3400, Tokyo, Japan). Samples were first adhered onto a double side adhesive tape folded on an aluminum mount. The mounted samples were there sputtered by gold particles under vacuum. The scanning was performed at an accelerating voltage of 15 KV and the images were observed for surface characters [23].

## 2.6. EVALUATION OF PNPs

### 2.6.1. Determination of drug loading

Nanoparticles equivalent to 30 mg of pure drug was dissolved in 100 ml of 6.8 pH phosphate buffer, followed by stirring. The solution was filtered through a 0.45 μ membrane filter, diluted and the absorbance of resultant solution was measured spectrophotometrically at 263 nm [24]. The drug content of the prepared nanoparticles was determined by using the following equation:

$$\text{Drug content (\%)} = \frac{\text{weight of drug in nanoparticles}}{\text{Total weight of nanoparticles}} \times 100$$

### 2.6.2. Determination of entrapment efficiency

The percentage entrapment efficiency was estimated by measuring amount of an entrapped drug in PNPs dispersion. PNPs dispersion was centrifuged at 10000 rpm for 45 min so as to settle the PNPs pellet. 1 ml of supernatant was dissolved in 10 ml of methanol, the solution was filtered and

amount of free drug in the supernatant was determined by measuring absorbance at 263 nm in UV spectrophotometer (UV 1700, Shimadzu AS, Japan) [25]. %EE was calculated from the following equation:

$$\text{Entrapment Efficiency (EE \%)} = \frac{\text{Amount of Drug in nanoparticles}}{\text{Total amount of Drug taken}} \times 100$$

### 2.6.3. In vitro drug release study for PNPs

The *in vitro* drug release study of PNPs was performed by Franz diffusion type cell. The study was performed at  $37 \pm 0.5$  °C, Receptor compartment of diffusion cell contained 20 ml of phosphate buffer (pH-7.4) solution and was constantly stirred by a magnetic stirrer at 100 rpm. Cellophane membrane (molecular weight cut off 10,000-12,000, Hi-Media, India), was employed as release barrier in between receptor and donor compartment which was previously soaked in distilled water. Samples were withdrawn on definite time intervals from sampling port of the diffusion cell and immediately replaced with an equal volume of fresh buffer. The amount of drug released was quantified using the High performance liquid chromatography (HPLC) method by directly injecting samples to the HPLC system at 263 nm [26-28].

### 2.6.4. Kinetic analysis of *in vitro* release data

The selection of best fit model (PCP Disso v2.08) was based on highest correlation coefficient values or determination coefficient ( $R^2$ ). To study the drug release mechanism from the nanoparticles, the following equation based on Korsmeyer-Peppas model was employed [29].

$$\frac{M_t}{M_\infty} = kt^n$$

Where,  $M_t/M_\infty$  = the fraction of drug released; t = time; k = constant.

The various mechanisms of drug release based on 'n' values are:

n = 0.5 - Case I transport (Fickian diffusion); 0.5 < n < 1 - Anomalous (non-Fickian) diffusion; n = 1 - Case II transport

(Zero order release); n > 1 - Super case II transport.

## 2.7. ESTABLISHMENT OF DESIGN SPACE

The ICH Q8 defines design space as “the multi dimensional combination and interaction of input variables and process parameters that have been demonstrated to provide assurance of quality”. Design space was generated using Design-Experiment Software 10 and constraints for the desired response were selected. The batch suggested by software was prepared using same procedure as described above and predicted value was compared with observed value [30].

## 3. RESULTS AND DISCUSSION

### 3.1 PREFORMULATION STUDIES

#### 3.1.1. FT-IR Studies

FTIR spectra of pure Rivastigmine Tartrate and its physical mixture depicted in Figure 1. From the spectra it was evident that there is no inter action between the drug and physical mixture.

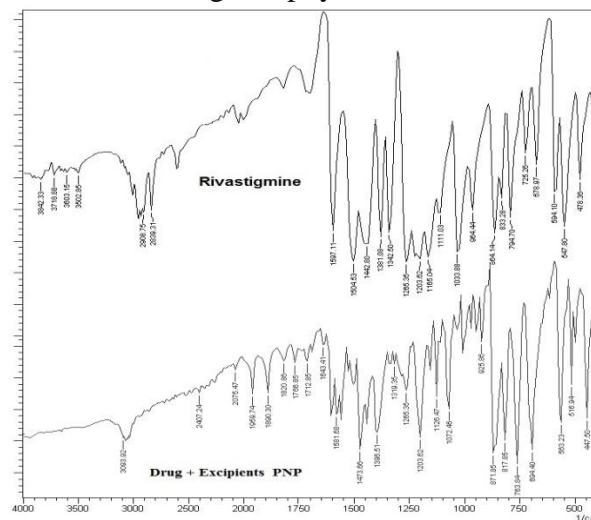
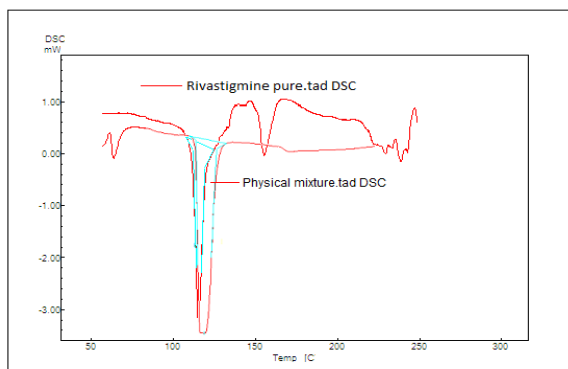


Figure 1. FT-IR spectra peaks of pure Rivastigmine Tartrate and physical mixture

#### 3.1.2. DSC Studies

DSC studies were carried out for pure Rivastigmine Tartrate and physical mixture. The results showed there is no evident shift in the peaks for pure drug and mixture. The results are showed in Figure 2.



**Figure 2.** DSC thermograms of pure Rivastigmine Tartrate and physical mixture

### 3.2. EXPERIMENTAL RESULTS

Design of experiments (DOE) is a scientific approach applied to understand the process in a larger way and to resolve how the input influences the response. In the present work,  $3^2$  factorial designs were applied to study the effect of variable on the selected responses. Every excipient is included to suit the needs of product use and processibility. By conducting a group of preliminary trials with relative ratio of the selected two components i.e. Glycol chitosan and Poloxamer 188 on the previous related experiences, the upper and the lower limits of each variable were defined (Table 3). To evaluate all the possible combination of excipients in the initial formulation system, a full factorial DoE of studies is required. Nine formulations (RP1-RP9) were prepared accordingly and analysed for their physical characteristics.

**Table 3. Variables in  $3^2$  factorial designs for PNPs**

Independent variables	Levels	
	Low (%)	High (%)
A: Glycol chitosan	0.2	0.4
B: Poloxamer 188	0.02	0.04
Dependent variables		
S1: Particle size (nm)		
S2: Entrapment efficiency (%)		
S3: Cumulative drug release (%)		

### 3.3. CHARACTERIZATION OF PNPs

#### 3.3.1. Determination of Particle size, Zeta potential and Polydispersity index

The nanoparticles size was most important factor for drug permeation through the skin. Particle size is often used to characterize the nanoparticles facilitation via skin and understanding of aggregation. In the case of large surface area, the attractive force between the particles increases and chance for possible aggregation in smaller sized particles. To overcome such aggregation, addition of a surfactant in the preparation was necessary. Poloxamer 188 appeared to be the most suitable surfactant for reducing aggregation between nanoparticles, as it suspends quickly after formation. Rivastigmine Tartrate loaded PNPs were evaluated for particle size, zeta potential and PDI. The results obtained are graphically represented in Figure 3, 4 and 5.

The formulations RP1–RP9 shows the particle size range between  $247 \pm 15$  nm and  $459 \pm 11$  nm. It indicates that the particle size increase with decrease in concentration of polymer.

The particle size data showed that the nanoparticle has submicron size and low polydispersity, which indicates relatively narrow size distribution.

The PDI of all formulations was found to be in the range of 0.374-0.719, which concluded that prepared nanoparticle was mono dispersed in nature.

Zeta potential higher than +30 mV indicates the stability of nanoparticles. The observed zeta potential for the prepared nanoparticles was range of  $35.81 \pm 3.4$  -  $50.36 \pm 2.7$  mV which confirms that the system remained stable without aggregation.



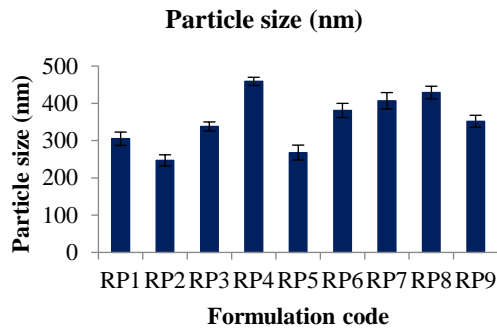


**Figure 3.** Average particle size (nm) of PNP (RP1- RP9)

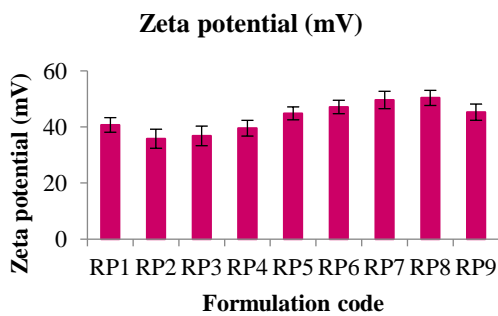


**Figure 4.** Zeta potential (mV) of PNP (RP1-RP9)

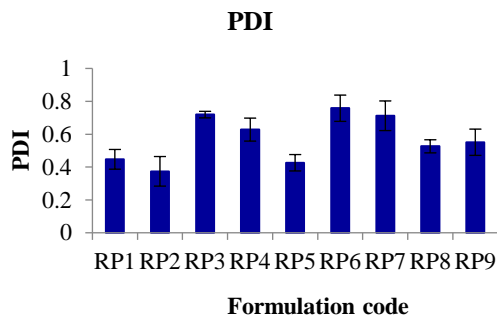


**Figure 5.** Polydispersity index of PNP (RP1-RP9)

### 3.3.2. Scanning Electron Microscopy (SEM)

The glycol chitosan nanoparticles have spherical shape with smooth surface. The surface morphology of formulated nanoparticles depends on a saturated solution of polymer produced irregular and rod shaped nanoparticles and the diffusion rate of solvent is varying fast and solvent may diffuse in to the aqueous phase before stabilization of nanoparticles and caused aggregation of nanoparticles. In the

formulation RP2, the polymer was fully saturated and the diffusion rate of solvent was minimal, leading to formation of smooth, spherical and homo-geneously distributed particles, which has smooth surface and the solvent was completely removal from the formulated nanoparticles (Figure 6).

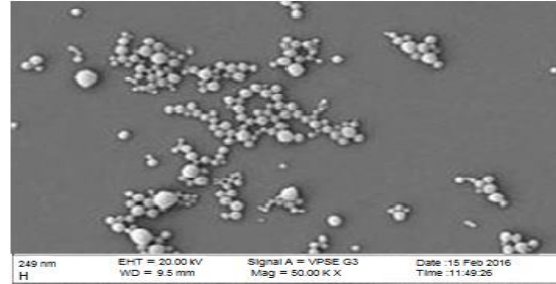


**Figure 6.** SEM image of Rivastigmine Tartrate polymeric nanoparticles

### 3.4. EVALUATION OF PNP

#### 3.4.1. Determination of drug loading and entrapment efficiency

The entrapment efficiency was the functional characteristic of polymer and surfactant etc. The entrapment efficiency was high in case of RP2 formulation due to high affinity of polymer and the surfactant. The low entrapment efficiency of the RP4 formulation was due to low affinity of polymer and the surfactant. The results of drug loading and entrapment efficiency for all the formulations are represented in Figure 7. It is observed from the results that the drug loading is in the range of  $16.91 \pm 0.7$  to  $21.41 \pm 1.5$  and entrapment efficiency in the range of  $41.62 \pm 1.5$  to  $51.47 \pm 1.8$ , indicating drug loading is satisfactory.

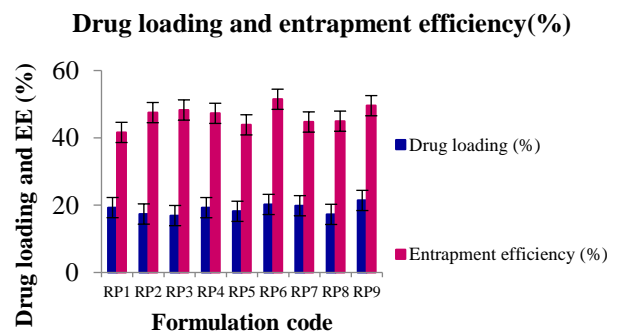


**Figure 7.** Drug loading and entrapment efficiency of PNP (RP1-RP9)

### 3.4.2. In vitro drug release studies

In vitro drug release studies were conducted for all formulations for 24 hrs and the results obtained are represented Figure 8 and 9. From the results, it was observed that, formulation RP-2 (97.81%) showed maximum release of the drug at the end of 24<sup>th</sup> h due to high concentration of the polymer and surfactant. Formulation RP-1, RP-3, RP-4, RP-5, RP-6, RP-7, RP-8 and RP-9 showed the release upto 94.91%, 94.18%, 86.72%, 96.1%, 91.55%, 90.14%, 87.8% and 92.17% respectively at the end of 24<sup>th</sup> h.

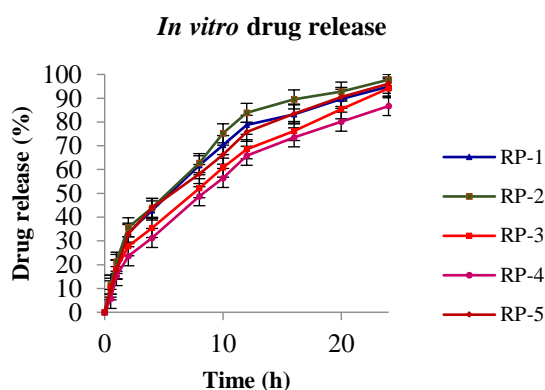


**Figure 8.** In vitro drug release profile of formulations (RP1-RP5)

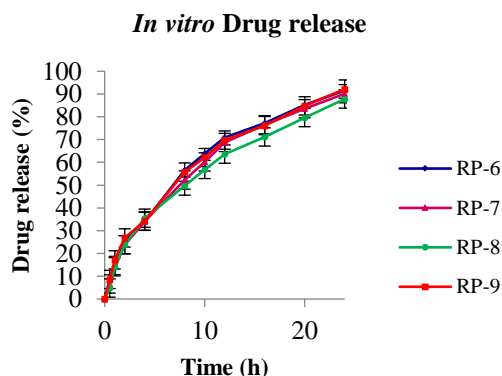


**Figure 9.** In vitro drug release profile of PNPs formulations (RP6-RP9)

### 3.4.3. Kinetic analysis of in vitro drug release for PNPs

The in vitro drug release data of all the formulations (RP1-RP9) was subjected to mathematical modelling. The best fit model with the highest correlation coefficient values or determination coefficients ( $R^2$ ) for the formulations RP-

1, RP-2, RP-3, RP-4, RP-5, RP-6, RP-7, RP-8 and RP-9 was found follow first order equation indicating the release of drug is directly proportional to concentration and the delivery system plays an important role in controlling the release of the drug. When these were fitted to the Korsmeyer and Peppas equation, the n values were >1 in all the cases, ranging from 1.1789 - 1.3132.

### 3.5. EXPERIMENTAL DESIGN OBSERVED RESPONSE IN 3<sup>2</sup> FACTORIAL DESIGN FOR RIVASTIGMINE TARTRATE PNPS

The application of factorial design yielded the following regression equations.

**A. Particle Size** = + 668.00000 - 255.00000 \* Polymer - 7916.66667

**B. \* Surfactant**

**C. Entrapment Efficiency** = + 32.60944 + 14.71667 \* Polymer + 318.66667 \* Surfactant

**D. Cumulative drug release** = + 63.11667 + 19.38333 \* Polymer + 579.16667 \* Surfactant

The polynomial regression results were expressed using Contour graphs, predicted & actual graphs and 3-D graphs (Figure 10 -12). The regression equation depicts that, the effect of polymer and surfactant on particle size. It clearly shows that at lower concentration of polymer and surfactant the particle size increased. A result of regression equation depicts that, the concentration of polymer and poloxamer-188 increases and the entrapment efficiency also increased. A result of regression analysis showed that, the concentration of polymer and surfactant increases and the drug release also increased. ANOVA for response surface linear model results were got significant for all responses. The  $R^2$  values were near to 1. Particle size 247, entrapment efficiency 51.57 and % cumulative drug release at 20<sup>th</sup> h 97.81% indicated high validity of models for experimental data.



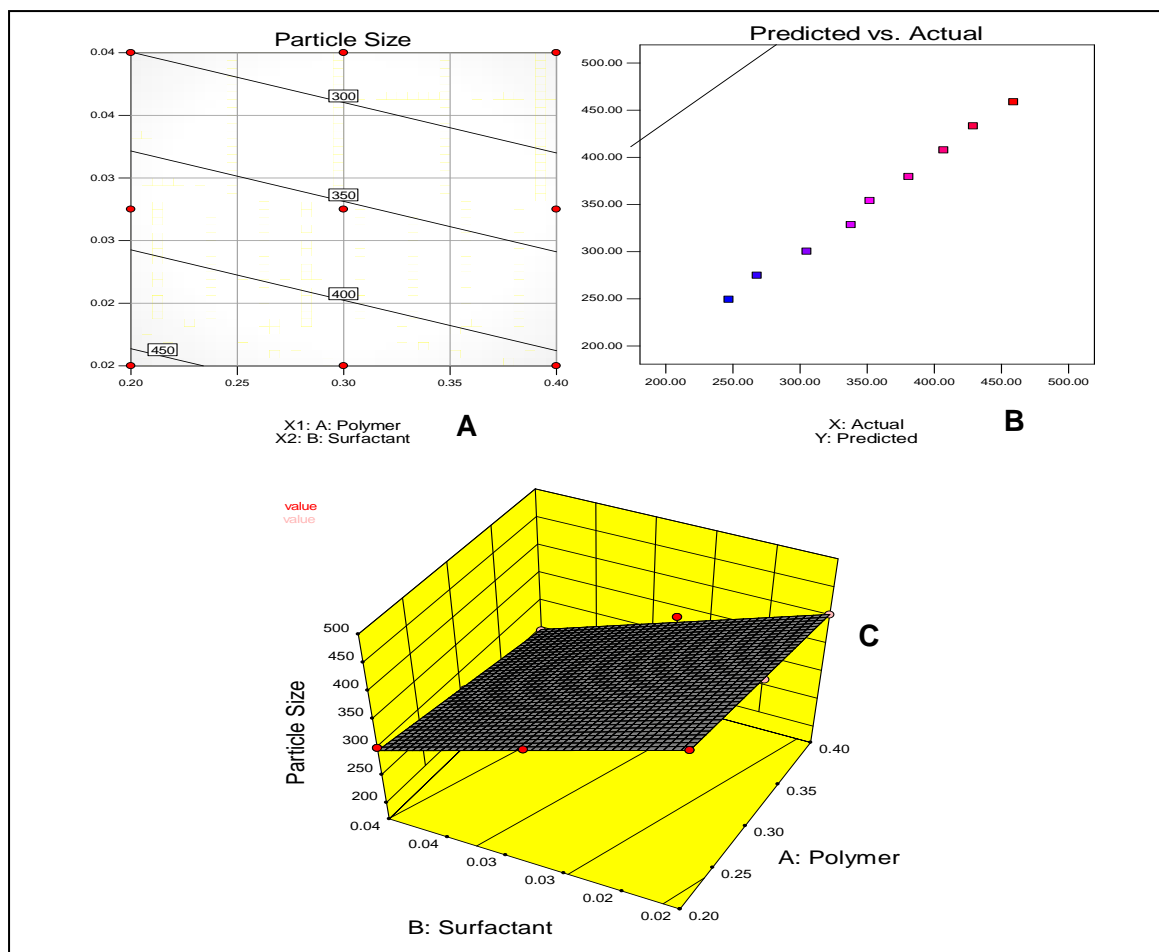


**Figure 10.** (A) Contour plot, (B) Predicted V/S actual plot and (C) Three-dimensional response surface plot depicting the impact of polymer and surfactant on particle size (nm) of PNPs respectively

**Table 4.** Check point analysis of optimized fomulations (RP-10) of PNPs

Value	Polymer (%)	Surfactant (%)	Particle size (nm)	Entrapment Efficiency (%)	% Cumulative drug release at 24 <sup>th</sup> h
<b>Predicted</b>	0.4	0.04	248.68	51.26	94.08
<b>Observed</b>	0.4	0.04	247	51.47	97.81
<b>Realtive error</b>			1.68	0.21	3.73

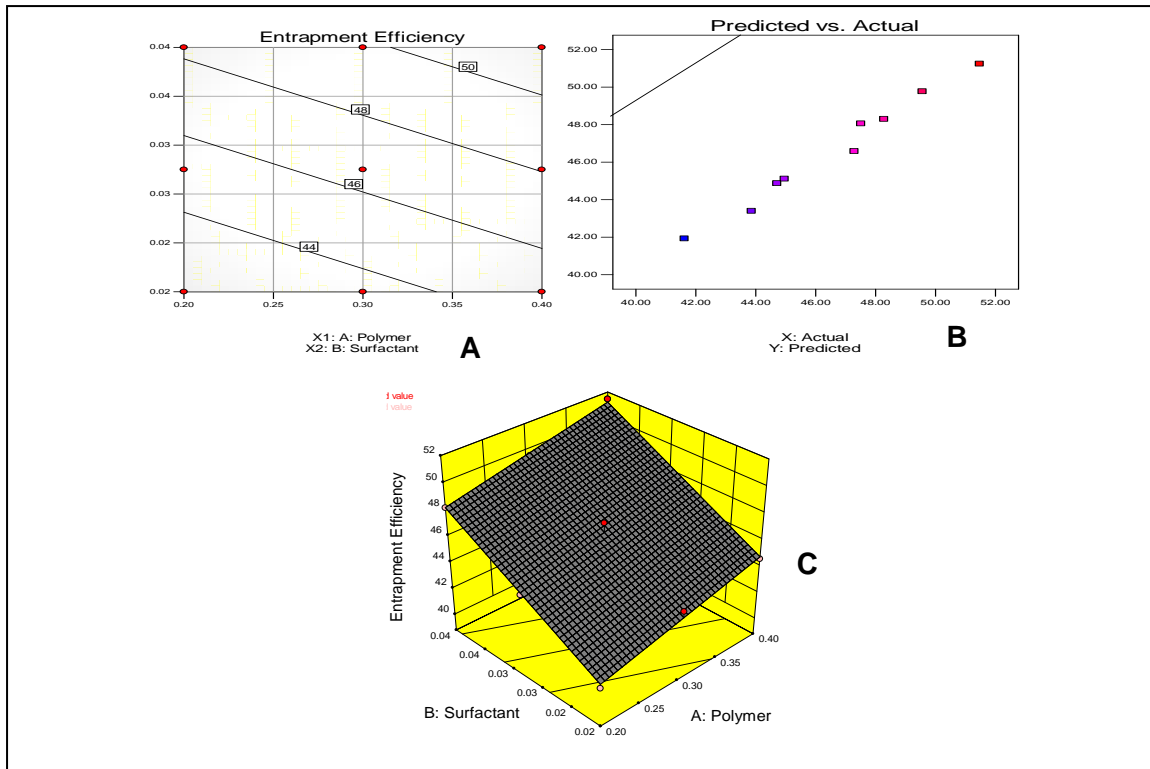


**Figure 11.** (A) Contour plot, (B) Predicted V/S actual plot and (C) Three-dimensional response surface plot depicting the impact of polymer & surfactant on entrapment efficiency (%) of PNPs respectively.

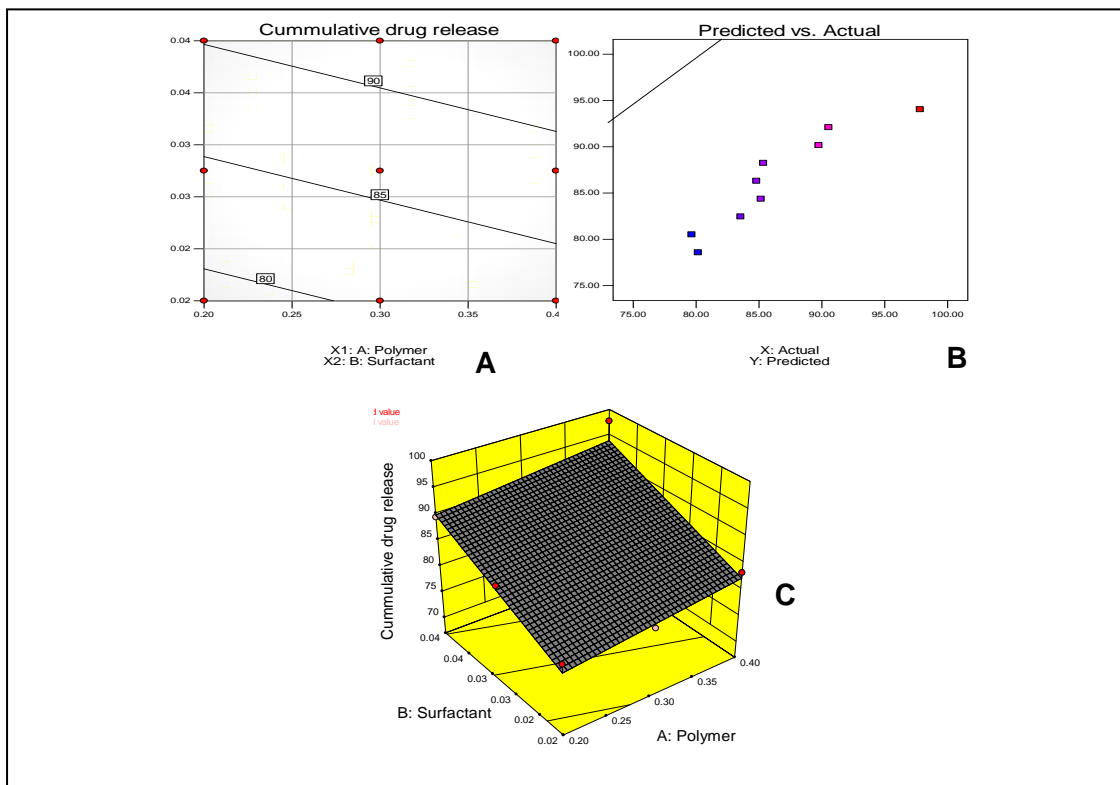


**Figure 12.** (A) Contour plot, (B) Predicted V/S actual plot and (C) Three-dimensional response surface plot depicting the impact of polymer and surfactant on drug release (%) of PNPs respectively.

### 3.6. CHECK POINT ANALYSIS AND OPTIMIZATION OF DESIGN (DESIGN SPACE)

To optimize all the responses with different targets, a multi-criteria decision method was employed (Figure 13). The optimized formulation (RP-10) was obtained by applying constraints as particle size=248.68 nm, EE = 51.26%, % cumulative drug release=94.08% on responses. These constrains were the same for all the formulations. Recommended concentrations of the factors were calculated by the DoE from above plots which has highest desirability near to 1.0. 0.49 % of lipid and 0.04% of surfactant was the optimum values of selected variables obtained using DoE. Desirability

and overlay plot of DoE gave optimum values of both factors, from that final formulation was prepared. The optimized formulation (RP-10) was prepared for check point analysis and evaluated. Particle size (R1), EE (R2) and % cumulative drug release (R3). The optimized formulation showed response variable as R1=247±15; R2= 51.47±1.8; R3= 97.81±0.26. Close agreement amongst predicted and observed values (Table 4) can be seen that is proved by desirability value of 0.905 with low relative errors (Figure 14). It demonstrates the reliability of the optimization method that was followed in the present study to formulate formulation as per 3<sup>2</sup> factorial designs.

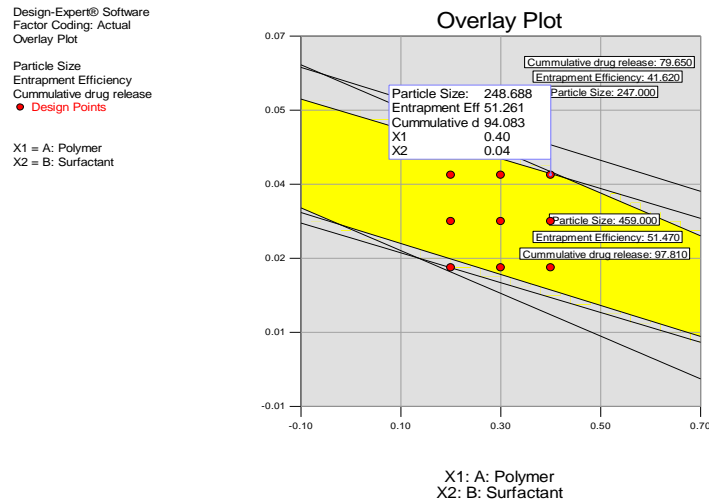


Figure 13. Overlay plot for optimization of PNPs

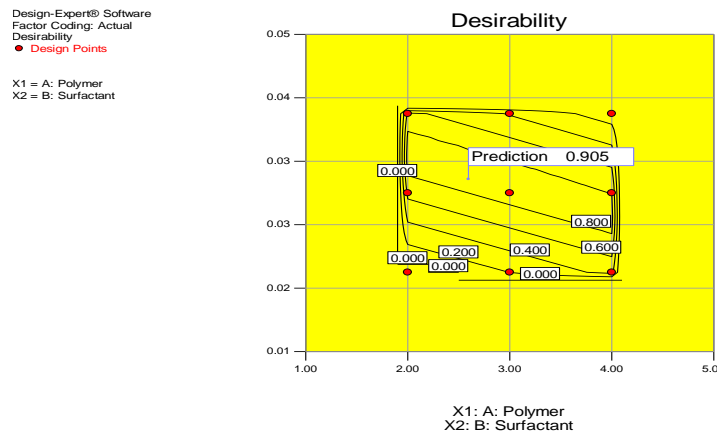


Figure 14. Desirability plot for optimization of PNPs

## CONCLUSION:

A QbD concept was used to understand the effect of different formulation and method variables on CQAs of PNPs such as particle size, entrapment efficiency and % cumulative drug release for 24 hours. Ishikawa diagram aided in the initial risk assessment for formulation improvement method. Full factorial design was employed using Design of Experiment 10.0 software. The optimized formulation prepared using the predicted level suggested by software showed the preferred response of particle size, entrapment efficiency and % cumulative drug release with desirability near to 1 confirming the appropriateness of the developed model. Therefore, statistical investigation of as PNPs formulation confirmed the potential of QbD concept in optimization of independent variables for PNPs preparation.

## REFERENCES:

1. M. L. Onor, M. Trevisiol, E. Aguglia, Rivastigmine in the treatment of Alzheimer's disease: an update, *Clin. Interv. Aging*. 2 (2007) 17-32.
2. J. A. R. Corey-Bloom, J. Veach, A randomized trial evaluating the efficacy and safety of ENA 713 (rivastigmine tartrate), a new acetylcholinesterase inhibitor, in patients with mild to moderately severe Alzheimer's disease, *Int. J. Geriatr. Psychopharmacol.* 1 (1998) 55-65.
3. M. Rosler, R. Anand, A. Cicin-Sain, S. Gauthier, Y. Agid, P. Dal-Bianco *et al.*, Efficacy and safety of rivastigmine in patients with Alzheimer's disease: international randomised controlled trial, *BMJ*. 3 (1999) 633-638.
4. G. Adler, S. Brassen, K. Chwalek, B. Dieter, M. Teufel. Prediction of treatment response to rivastigmine in Alzheimer's dementia, *J. Neurol. Neurosurg. Psychiatry*. 75 (2004) 292-294.
5. N. R. Cutler, Mancione *et al.*, Dose-dependent CSF acetylcholinesterase inhibition by SDZ ENA 713 in Alzheimer's disease, *Acta Neurol. Scand.* 97 (1998) 244-250.
6. A. Enz, A. Chappuis, A. Dattler, A simple, rapid and sensitive method for simultaneous determination of rivastigmine and its major metabolite NAP 226-90 in rat brain and plasma by reversed-phase liquid chromatography coupled to electrospray ionization mass spectrometry, *Biomed Chromatogr.* 18 (2004) 160-166.
7. G. Lefevre, G. Sedek, S. S. Jhee, M. T. Leibowitz, H. L. Huang, A. Enz *et al.*, Pharmacokinetics and pharmacodynamics of the novel daily rivastigmine transdermal patch compared with twicedaily capsules in Alzheimer's disease patients, *Clin. Pharmacol. Ther.* 83 (2008) 106-114.
8. M. C. Chou, Yang, Concentrations of rivastigmine and NAP 226-90 and the cognitive response in Taiwanese Alzheimer's disease patients, *J. Alzheimers Dis.* 31 (2012) 857-864.
9. A. Olad, R. H. Azar, A. A. Babaluo, Investigation on the mechanical and thermal properties of intercalated epoxy/layered silicate nanocomposites, *Int. J. Polym. Mater. Polym. Biomater.* 61 (2012) 1035-1049.
10. A. Kausar, S. T. Hussain, Azo-polymer based hybrids reinforced with carbon nanotubes and silver nanoparticles: solution and melt processing, *J. Polym. Mater. Polym. Biomater.* 63 (2014) 207-212.
11. N. Mehwish, A. Kausar, M. Siddiq, Advances in polymer-based nanostructured membranes for water treatment, *Polym. Plast. Technol. Eng.* 53 (2014) 1290-1316.
12. R. Francis, N. Joy, E. P. Aparna, R. Vijayan Polymer grafted inorganic nanoparticles, preparation, properties, and applications: A review, *Polym. Rev.* 54 (2014) 268-347.
13. S. S. Lateef, A. Vinayak, Quality-by-Design Approach to Stability Indicating Method Development for Linagliptin

- Drug Product, [cited 2017 Jan 11]. Available from: <http://www.agilent.com/cs/library/applications/5991-3834EN.pdf>.
14. National Centre for Biotechnology Information. PubChem Compound Database; CID=6918078. Emtricitabine | C<sub>8</sub>H<sub>10</sub>FN<sub>3</sub>O<sub>3</sub>S - PubChem [Internet]. [Cited 2017 Jan 11]. Available from: <https://pubchem.ncbi.nlm.nih.gov/compound/6918078#section=Top>.
  15. J. Maguire, D. Peng, How to Identify Critical Quality Attributes and Critical Process Parameters, 2005 [cited 2017 Jan 11]. Available from: <http://pqri.org/wp-content/uploads/2015/10/01-How-to-identify-CQA-CPP-CMA-Final.pdf>.
  16. S. Karmarkar, R. Garber, Y. QbD-Based Development of Stability Indicating HPLC Method for Drug and Impurities, J. Chromatogr. Sci. 17 (2011) 49.
  17. A. Homayouni, Garekani, Preparation and characterization of celecoxib solid dispersions; comparison of poloxamer-188 and PVP-K30 as carriers, Iranian J. Medical Sci. 17 (2014) 322.
  18. S. S. Bahulkar, N. M. Munot, S. S. Surwase, Synthesis, characterization of thiolated karaya gum and evaluation of effect of pH on its mucoadhesive and sustained release properties, Carbohydr. Polym. 130 (2015) 183-190.
  19. K. S. Rakesh, S. Navneet, R. Sudha, H. G. Shivkumar, Solid lipid nanoparticles as a carrier of metformin for transdermal delivery, Int. J. Drug Deliv. 5 (2013) 137-145.
  20. J. Malakara, A. K. Nayak, Formulation and statistical optimization of multiple unit ibuprofen loaded buoyant system using 2<sup>3</sup> factorial design, Chem. Eng. Res. Des. 90 (2012) 1834-1846.
  21. G. Singh, Devi, Response surface methodology and process optimization of sustained release pellets using taguchi orthogonal array design and central composite design, J. Adv. Pharm. Tech. Res. 3 (2012) 30-40.
  22. N. Chivate, S. Patil, J. Saboji, A. Chivate, Formulation and optimization of telmisartan solid dispersions by box-behken design, Int. J. Pharm. Sci. Health Care. 3 (2012) 33-47.
  23. A. Kumar, K. Sawant, Application of multiple regression analysis in optimization of anastrozole-loaded PLGA nanoparticles, J. Microencapsul. 31 (2014) 105-114.
  24. R. D. Deshpande, D. V. Gowda, N. Mahammed, Design of Pistacia lentiscus (mastic gum) controlled release spheroids and investigating the influence of roll compaction, Ind. Crops Prod. 44 (2012) 603-610.
  25. R. Paliwal, S. Rai, B. Vaidya, K. Khatri, A. Goyal *et. al.*, Effect of lipid core material on characteristics of solid lipid nanoparticles for oral lymphatic delivery, Nanomed. Nanotech. Biol. Med. 5 (2009) 184-191.
  26. M. P. Gowrav, H. Umme, H. G. Shivkumar *et. al.*, Polyacrylamide grafted guar gum based glimepiride loaded pH sensitive pellets for colon specific drug delivery: fabrication and characterization, RSC Adv. 5 (2015) 80005-80013.
  27. Y. Hua, X. Jianga, Preparation and drug release behaviours of nimodipine-loaded poly (caprolactone)-poly (ethyleneoxide)-poly lactide amphiphilic copolymer nanoparticles, Biomaterials. 24 (2003) 2395-2404.
  28. L. K. Omay, Formulation and characterization of solid lipid nanoparticles for Transdermal delivery of Testosterone, Int. J. Pharm. Sci. Res. 5 (2014) 323-328.
  29. P. Costa, J. M. S. Lobo, Modeling and comparison of dissolution profiles, Eur. J. Pharm. Sci. 13 (2001) 123-133.
  30. P. Mitali, S. Krutika, A Quality by Design Concept on Lipid Based Nanoformulation Containing Antipsychotic Drug: Screening Design and Optimization using Response Surface Methodology, J. Nanomed. Nanotechnology. 8 (2017) 2-11.